Organic & Biomolecular Chemistry

Cite this: *Org. Biomol. Chem.*, 2012, **10**, 1493

www.rsc.org/obc

COMMUNICATION

Probing the functional limits of the norepinephrine transporter with self-reporting, fluorescent stilbazolium dimers†

Erika L. Smith,[a,b] Adrienne S. Brown,[a] Edward Adjaye-Mensah[a] and James N. Wilson*[a]

Received 25th October 2011, Accepted 29th November 2011
DOI: 10.1039/c2ob06796j

A series of stilbazolium dimers were synthesized and investigated as sterically demanding ligands targeting the norepinephrine transporter (NET). The environmentally sensitive fluorescence of the dyes enables their use as self-reporting ligands; binding to and displacement from NET can be monitored by fluorescence microscopy.

Norepinephrine (NE) is a chemical messenger found in the both the periphery and the central nervous system (CNS). In the CNS, NE plays key roles in regulating mood, stress responses, learning, memory and wake–sleep cycles.[1–3] The norepinephrine transporter (NET) is responsible for removing NE from the synaptic cleft and extracellular milieu following neurotransmitter release. NET is the target of multiple pharmacotherapies including desipramine, duloxetine and milnacipran, highlighting its regulatory function (or dysregulation) in numerous disorders. In addition to its native substrate, NET has been shown to bind and transport synthetic analogues of neurotransmitters and neurotoxins.[4–6] For example the binding and transport of a cationic probe, ASP^+, was reported by DeFelice,[5] and recently we described a related stilbazolium dye, $HNEP^+$, that is also transported by NET.[6] Both of these fluorophores are relatively rigid and significantly larger than NE (Chart 1). This ability to bind and transport bulky substrates raises questions regarding the functional limits of NET (*i.e.* What are the maximum substrate dimensions?) with significant implications on drug design.

We have examined a series of bifunctional cationic fluorophores consisting of two stilbazolium dyes (**1–4**, Chart 1) tethered by a flexible six-carbon linker as probes of the binding and transport limits of NET. These dimer constructs are greater than 30.0 Å in length in an unfolded conformation compared to 8.8 Å for NE. However, we anticipated that the dimers could exploit the close proximity of the two binding pockets predicted in NET homology models.[7,8] Based on these models as well as the crystal structures of the leucine transporter complexed with L-leucine and several reuptake inhibitors, we selected a six-carbon chain as the flexible linker between the two chromophores. The stilbazolium dyes used to construct **1–4** possess a range of NET activities that may be monitored spectroscopically or by confocal microscopy. $HNEP^+$ and ASP^+, the chromophores embedded in **1** and **4** respectively, bind to and are transported by NET. NEP^+, the monomer component of **2**, was reported to bind to NET, but no evidence of transport by NET was observed.[6] Neither binding, nor uptake of MSP^+, the corresponding methylstilbazolium derivative of **3**, was detected.[6]

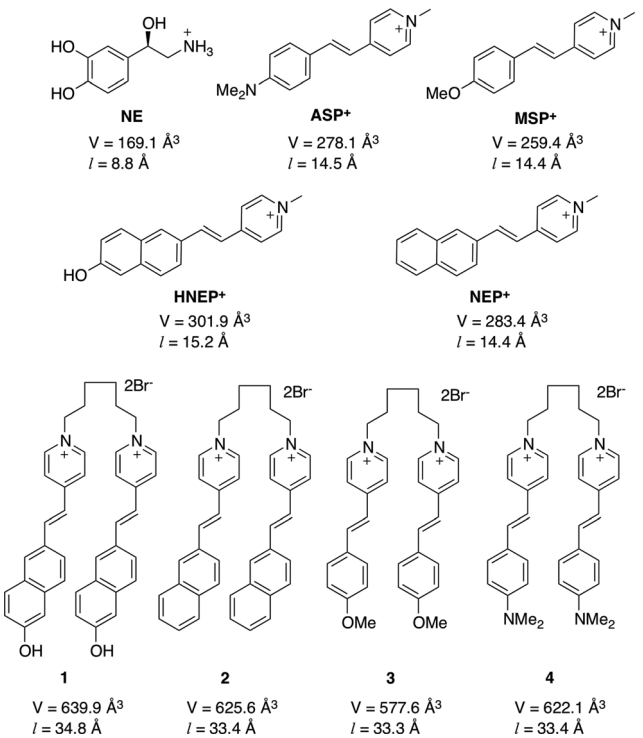

Chart 1 Structures and physical dimensions of NE (protonated form), stilbazolium dyes ASP^+, MSP^+, $HNEP^+$, NEP^+ and bifunctional dyes **1–4**.

Probes **1–4** were synthesized by a double Knoevenagel condensation[9] of N,N′-(1,6-hexanediyl)bis(4-methylpyridinium) dibromide with the appropriate aromatic aldehyde; the synthesis

[a]*Department of Chemistry, University of Miami, 1301 Memorial Drive, Coral Gables, FL 33124, USA. E-mail: jnwilson@miami.edu; Fax: +1 305 284 4571; Tel: +1 305 284 2619*
[b]*Present address: Princeton University, 2457 Frist Center, Princeton, NJ 08544, USA*

†Electronic supplementary information (ESI) available: ^{1}H-NMR, ^{13}C-NMR, IR, MP, HRMS and ^{1}H-NMR spectra for **1** and **2**; details of cell preparation, confocal microscopy, and molecular docking experiments. See DOI: 10.1039/c2ob06796j

Table 1 Summary of photophysical parameters for **1–4**

	$\lambda_{max,\ abs}$ [a] (nm)	ε [a] (M^{-1}, cm^{-1})	$\lambda_{max,\ em}$ [a] (nm)	Φ_{em} [a]	$\lambda_{max,\ em}$ [b] (nm)	Φ_{em} [b]	I_{oct}/I_{PBS}
1	425	65 000	545	2.2×10^{-1}	470	1.6×10^{-3}	137
2	323	39 000	462	8.0×10^{-2}	494	5.7×10^{-3}	14
3	386	67 000	467	1.0×10^{-2}	476	3.6×10^{-3}	3.2
4	484	79 000	581	1.6×10^{-1}	—[c]	$<1.0 \times 10^{-3}$	>160

[a] In octanol; [b] In PBS; [c] Too weak to determine

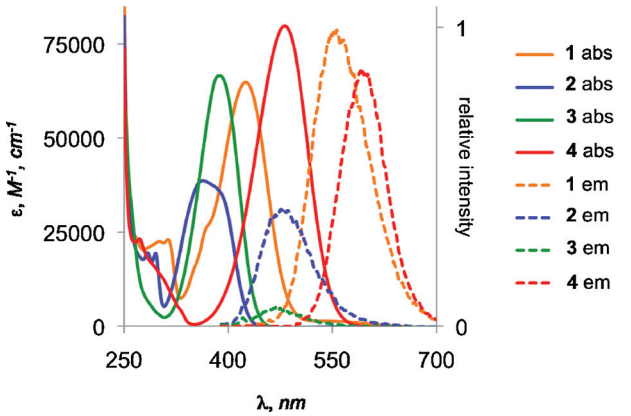

Fig. 1 Absorption (solid lines) and emission (dashed lines) of probes **1–4** taken in octanol.

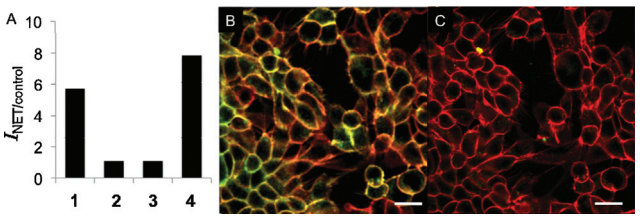

Fig. 2 Probes **1** and **4** exhibit greater association with NET-expressing HEK293 cells, when compared to controls, as determined by the emission intensity (panel A) following identical treatment conditions (500 nM, 30 min). Panel B depicts the colocalization of **4** (green channel) with a cell membrane dye (CellMask Deep Red, red channel); areas of overlap appear in yellow. Addition of desipramine, (panel C, 2 μM final concentration) results in displacement of **4** indicating NET is the cell membrane target of the dimer probe. Scale bar is 10 μm.

of **3** and **4** has previously been described.[10] The products were obtained as brightly colored crystalline solids following crystallization from methanol and were characterized by ^{1}H-NMR, ^{13}C-NMR, HRMS, IR, UV-vis and fluorescence spectroscopy.†

Table 1 summarizes the optical properties of **1–4**. The dyes possess $\lambda_{max,\ abs}$ ranging from 363 nm (**2**) to 484 nm (**4**), which correlates well with the presence of electron donating auxochromes. The broad, amorphous peaks observed in the UV-vis spectra are characteristic of intramolecular charge transfer (ICT) transitions that result from the presence of the strongly electron withdrawing pyridinium moiety. As a consequence, the excited states of **1–4** should be highly sensitive to solvent polarity, a behavior observed with ASP^{+} which is weakly or non-emissive in methanol or aqueous solutions but exhibits good to moderate quantum yields in less polar solvents.[5,11] Fluorescence spectroscopy reveals that **1–4** possess similar polarity dependant emission (Fig. 1, Table 1). In phosphate buffered saline (PBS), probes **1–4** show weak or no emission upon photoexcitation. However, in octanol, emission is significantly enhanced with greater than 100-fold increases observed for **1** and **4**. This behavior is ideal for imaging applications and monitoring binding or transport as the probe "turns-on" when bound or accumulated intracellularly.[11]

We screened **1–4** against HEK293 cells stably expressing hNET[12] and compared the emission intensities against untransfected HEK293 cells, which served as controls. Cells were treated with 500 nM solutions of the dyes for 30 min then imaged by confocal microscopy with excitation *via* 405 nm or 488 nm laser lines; details of imaging experiments are provided in the ESI.† The ratio of intensities for NET and control cells was used to determine if the probes associated with the cells in an NET-dependent manner. The largest ratios were observed for **1** and **4** (Fig. 2A), suggesting these stilbazolium dimers interact with NET, while little or no association was detected for **2** and **3**.

Dual-labelling experiments provide further evidence supporting the notion that **1** and **4** bind to NET (Fig. 2B, C). hNET-HEK293 cells were treated with a membrane-targeting dye (CellMask Deep Red, Invitrogen), then with **1** (2 μM) or **4** (500 nM). The membrane dye was imaged in the red channel (λ_{ex} = 633 nm), and the NET-targeting dyes were imaged in the green channel (λ_{ex} = 405 nm for **1** or 488 nm for **4**). The overlaid images show that **4** colocalizes to the plasma membrane; colocalization is evident as the areas in yellow in Fig. 2B (images for **1** in Fig S3†). Subsequent addition of desipramine (2 μM final concentration), a norepinephrine reuptake inhibitor (K_i = 5.5 nM),[13] to the fluorophore-containing media results in complete displacement of **1** and **4** with concomitant loss of emission intensity (Fig. 2C). Control HEK293 cells treated under identical conditions show no evidence of **1** or **4** colocalized to the plasma membrane.

The binding and desipramine-induced displacement of **1** and **4** were examined in further detail for comparison with the model compounds HNEP^{+} and ASP^{+} (Fig. 3). Both HNEP^{+} and ASP^{+} exhibit two distinct activity phases in accordance with earlier studies on ASP^{+}.[5] The first phase, ascribed to substrate binding to NET, is characterized by a rapid rise in emission intensity over the first 10 s following introduction of the dye. The second phase corresponds to substrate transport and intracellular accumulation. Neither **1** nor **4** possess an NET-dependent transport phase, even when monitored over longer time periods (up to 15 min). Dimers **1** and **4** exhibit binding saturation kinetics at approximately half the rate compared to the HNEP^{+} and ASP^{+} (Table 2). The off-rates are also lower for the dimers. Several

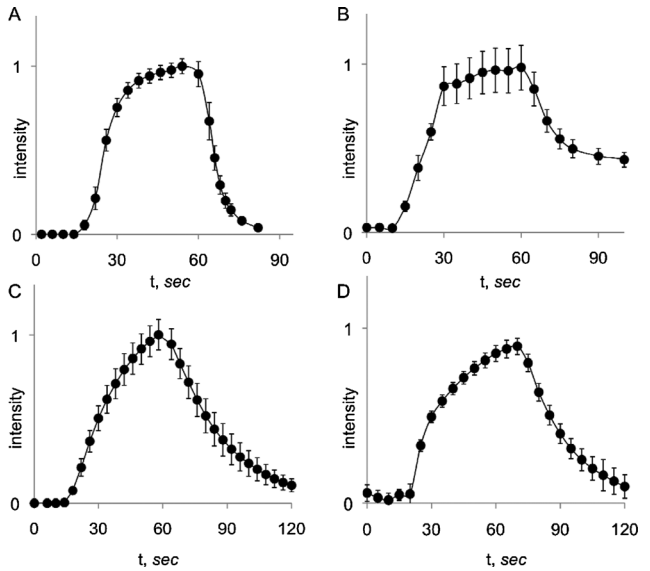

Fig. 3 Binding and displacement curves of ASP^+ (A), $HNEP^+$ (B), **4** (C), and **1** (D). Probes were introduced at $t = 15$ s to produce a final concentration of 500 nM (ASP^+, **4**) or 2 μM ($HNEP^+$, **1**); desipramine was introduced between $t = 55$ s and 65 s to produce a final concentration of 2 μM. Observed on and off rates were slower for **1** and **4** compared to ASP^+ and $HNEP^+$. Data points represent the mean of four independent experiments for each compound ± s.e.m.

Table 2 Summary of binding and displacement kinetics

	k_{on} $(s^{-1})^a$	k_{off} $(s^{-1})^a$
1	$2.9 \times 10^4 \pm 7.0 \times 10^3$	$3.7 \times 10^{-2} \pm 3.0 \times 10^{-3}$
$HNEP^+$	$4.8 \times 10^4 \pm 7.2 \times 10^3$	$7.3 \times 10^{-2} \pm 1.2 \times 10^{-2}$
4	$1.2 \times 10^5 \pm 1.0 \times 10^4$	$4.0 \times 10^{-2} \pm 5.0 \times 10^{-3}$
ASP^+	$2.7 \times 10^5 \pm 7.0 \times 10^4$	$1.8 \times 10^{-1} \pm 5.0 \times 10^{-3}$

[a] Calculated from time dependent emission intensities of four independent experiments using Prism (GraphPad Software).

factors likely contribute to the slower rates observed for the dimers. First, they may exist in a folded or sandwich conformation that does not allow for binding to NET. Secondly, binding to NET may require a conformational change to accommodate the bulkier dimer constructs.

Molecular docking, utilizing the NET-homologous leucine transporter (LeuT) crystallized with bound substrate and desipramine (PDB ID: 2QJU),[14] provides some insight into the potential binding modes of the dimers (Fig. 4).[15] While the details of probe binding to NET *versus* LeuT may differ, the observed activity and displacement of **1**, **4**, ASP^+ and $HNEP^+$ provide empirical support for several aspects of the predicted binding modes. As expected from their transport activity, ASP^+ and $HNEP^+$ were found to overlap with the substrate-binding site deep in the LeuT permeation pathway. Both probes also overlap, to a small degree, with the more exposed desipramine-binding site, which is in agreement with the observed inhibitor-induced displacement. Thus, **1** and **4** were found to overlap with both the substrate and inhibitor binding pockets. The lack of transport activity may be linked to this binding conformation as the dimers abut the regions of transmembrane domains 1 and 6 that are predicted to close during substrate transport.[16]

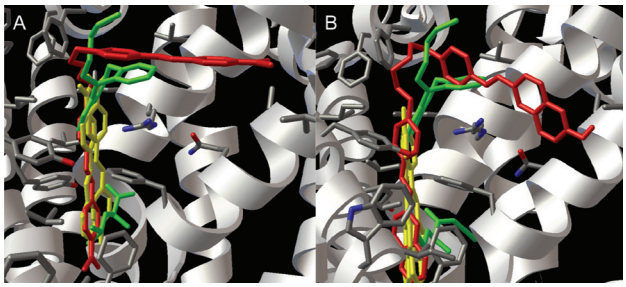

Fig. 4 Molecular docking (AutoDock Vina)[15] of probes in the NET-homologous LeuT.[16] At left, ASP^+ (in yellow) overlaps with the binding site of Leu (at bottom in green) and partially with the desipramine (at top in green) binding site. Dimer probe **4** (in red) shows more extensive overlap with the desipramine binding site and extends towards transmembrane domains 1 and 6. $HNEP^+$ and **1** exhibit similar binding modes as shown at right ($HNEP^+$ in yellow, **1** in red).

Conclusions

We have probed the functional limits of NET utilizing sterically demanding stilbazolium dimers that exhibit "turn-on" fluorescence. From these studies, we conclude that NET is capable of binding ligands with significantly larger dimensions than NE, yet transport is likely limited to ligands that occupy the substrate-binding pocket with minimal overlap of the inhibitor-binding site. Beyond the current studies, probes **1** and **4** may be utilized as markers of monoamine transporter distribution, serving as alternatives to antibody labelling. Additionally, they may be useful for studying NET conformations by measuring FRET with the aromatic residues lining the binding pockets. This information could provide insights into binding site topology with implications for future drug design.

Acknowledgements

We thank Prof. R. Blakely for providing the hNET-HEK293 cells, Prof. R. Prabahakar and Arghya Barman (UM, Chemistry) for their assistance with molecular docking, and the National Science Foundation for providing funds towards the purchase of an LC-ESI-MS (CHE-0946858). This work was supported by a grant from the James & Esther King Biomedical Research Program (1KF08).

Notes and references

1 H. A. Mitchell and D. Weinshenker, *Biochem. Pharmacol.*, 2010, **79**, 801.
2 A. B. Hains and A. F. Arnsten, *Learn. Mem.*, 2008, **15**, 551.
3 K. Tully and V. Y. Bolshakov, *Mol. Brain*, 2010, **3**, 15.
4 D. Hadrich, F. Berthold, E. Steckhan and H. Bönisch, *J. Med. Chem.*, 1999, **42**, 3101.
5 J. W. Schwartz, R. D. Blakely and L. J. DeFelice, *J. Biol. Chem.*, 2003, **278**, 9768.
6 A. S. Brown, L. M. Bernal, T. L. Micotto, E. L. Smith and J. N. Wilson, *Org. Biomol. Chem.*, 2011, **9**, 2142.
7 A. W. Ravna, I. Sylte and S. G. Dahl, *J. Mol. Model.*, 2009, **15**, 1155.
8 F. A. Paczkowski, I. A. Sharpe, S. Dutertre and R. J. Lewis, *J. Biol. Chem.*, 2007, **282**, 17837.
9 E. Knoevenagel, *Ber. Dtsch. Chem. Ges.*, 1898, **31**, 2596.

10 J. K. Mishra, P. K. Behera, S. K. Parida and B. K. Mishra, *Indian J. Chem., Sect. B.*, 1992, **31**, 118.
11 A. P. de Silva, H. Q. N. Gunaratne, T. Gunnlaugsson, A. J. M. Huxley, C. P. McCoy, J. T. Rademacher and T. E. Rice, *Chem. Rev.*, 1997, **97**, 1515.
12 A. Galli, L. J. DeFelice, B. J. Duke, K. R. Moore and R. D. Blakely, *J. Exp. Biol.*, 1995, **198**, 2197.
13 F. A. Paczkowski and L. J. Bryan-Lluka, *Naunyn-Schmiedebergs Arch. Pharmacol.*, 2002, **365**, 312.
14 Z. Zhou, J. Zhen, N. K. Karpowich, R. M. Goetz, C. J. Law, M. E. A. Reith and D.-N. Wang, *Science*, 2007, **317**, 1390.
15 O. Trott and A. J. Olson, *J. Comput. Chem.*, 2010, **31**, 455–461.
16 A. Yamashita, S. K. Singh, T. Kawate, Y. Jin and E. Gouaux, *Nature*, 2005, **437**, 215.

